

Activities of Secreted Aryl Alcohol Quinone Oxidoreductases from *Pycnoporus cinnabarinus* Provide Insights into Fungal Degradation of Plant Biomass

Yann Mathieu,^{a,b} Francois Piumi,^{a,b} Richard Valli,^{a,b} Juan Carro Aramburu,^c Patricia Ferreira,^d Craig B. Faulds,^{a,b} Eric Record^{a,b}

INRA, UMR 1163 Biotechnologie des Champignons Filamenteux, Polytech Marseille, Marseille, France^a; Aix Marseille Université, UMR 1163 Biotechnologie des Champignons Filamenteux, Polytech Marseille, Marseille, France^b; Biotechnology for Lignocellulosic Biomass Lab, Centro de Investigaciones Biológicas, Madrid, Spain^c; Departamento de Bioquímica y Biología Molecular y Celular, Instituto de Biocomputación y Física de Sistemas Complejos, Universidad de Zaragoza, Zaragoza, Spain^d

Auxiliary activities family 3 subfamily 2 (AA3_2) from the CAZy database comprises various functions related to ligninolytic enzymes, such as fungal aryl alcohol oxidases (AAO) and glucose oxidases, both of which are flavoenzymes. The recent study of the *Pycnoporus cinnabarinus* CIRM BRFM 137 genome combined with its secretome revealed that four AA3_2 enzymes are secreted during biomass degradation. One of these AA3_2 enzymes, scf184803.g17, has recently been produced heterologously in *Aspergillus niger*. Based on the enzyme's activity and specificity, it was assigned to the glucose dehydrogenases (*P. cinnabarinus* GDH [PcGDH]). Here, we analyze the distribution of the other three AA3_2 enzymes (scf185002.g8, scf184611.g7, and scf184746.g13) to assess their putative functions. These proteins showed the highest homology with aryl alcohol oxidase from *Pleurotus eryngii*. Biochemical characterization demonstrated that they were also flavoenzymes harboring flavin adenine dinucleotide (FAD) as a cofactor and able to oxidize a wide variety of phenolic and nonphenolic aryl alcohols and one aliphatic polyunsaturated primary alcohol. Though presenting homology with fungal AAOs, these enzymes exhibited greater efficiency in reducing electron acceptors (quinones and one artificial acceptor) than molecular oxygen and so were defined as aryl-alcohol:quinone oxidoreductases (AAQOs) with two enzymes possessing residual oxidase activity (PcAAQO2 and PcAAQO3). Structural comparison of PcAAQO homology models with *P. eryngii* AAO demonstrated a wider substrate access channel connecting the active-site cavity to the solvent, explaining the absence of activity with molecular oxygen. Finally, the ability of PcAAQOs to reduce radical intermediates generated by laccase from *P. cinnabarinus* was demonstrated, shedding light on the ligninolytic system of this fungus.

Auxiliary activities (AA) are a widespread group of catalytic modules involved in plant cell wall degradation. They were first introduced in 2013 into the carbohydrate-active enzymes (CAZy [www.cazy.org]) database (1). This AA class encompasses and extends an earlier classification dedicated to fungal ligninolytic enzymes and comprises 10 families, some of which have subfamilies (2). The AA family group enzymes possess the potential ability to help the original carbohydrate-active enzymes gain access to the carbohydrates embedded in the plant cell wall. Lignin, the main noncarbohydrate structural component of plant cell walls, consists of an intricate network of aromatic compounds forming a strong, hydrophobic, insoluble barrier closing access to the carbohydrates. Microorganisms have therefore set up different strategies to either modify or degrade lignin as a first step to gain access to the carbohydrate moiety and convert it into an energy source (3).

In this new AA classification, family AA3 belongs to the glucose-methanol-choline (GMC) oxidoreductase family first defined by Cavener (4). AA3 enzymes are flavoproteins containing a flavin adenine dinucleotide (FAD)-binding domain and can be subdivided into four subfamilies: AA3_1 (mostly covering cellobiose dehydrogenase), AA3_2 (including both aryl alcohol oxidase and glucose 1-oxidase), AA3_3 (alcohol oxidase), and AA3_4 (pyranose 2-oxidase). Within the AA3_2 subfamily, aryl alcohol oxidases (AAOs) catalyze the oxidative dehydrogenation of several aromatic and aliphatic polyunsaturated alcohols with an α -carbon primary hydroxyl group, with the concomitant reduction of O_2 to H_2O_2 required for class II peroxidases to oxidize

lignin. They were first described in *Polystictus versicolor* (5). AAO activity was later detected in different fungi, including *Pleurotus* species (6–9), *Fusarium solani* (10), *Rigidoporus microporus* (synonym, *Fomes lignosus*) (11), *Bjerkandera adusta* (12, 13), and *Botrytis cinerea* (14). The simultaneous production of AAO and lignin peroxidase (LiP) in *B. adusta* (15) and of AAO and versatile peroxidase in *Pleurotus* cultures (16) supports AAO involvement in lignin degradation. AAO localization was investigated during wheat straw degradation by *Pleurotus eryngii* under solid-state fermentation conditions. Although the enzyme was initially located in the hyphal sheath, AAOs can penetrate the partially degraded, or modified, cell walls of phloem and parenchyma and also the more densely lignified sclerenchymatic tissues to act synergistically with other lignin-degrading enzymes (17). An extracellular AAO has also been characterized in the maize parasitic fungus

Received 24 November 2015 Accepted 8 February 2016

Accepted manuscript posted online 12 February 2016

Citation Mathieu Y, Piumi F, Valli R, Aramburu JC, Ferreira P, Faulds CB, Record E. 2016. Activities of secreted aryl alcohol quinone oxidoreductases from *Pycnoporus cinnabarinus* provide insights into fungal degradation of plant biomass. Appl Environ Microbiol 82:2411–2423. doi:10.1128/AEM.03761-15.

Editor: A. A. Brakhage, HKI and University of Jena

Address correspondence to Yann Mathieu, yann.mathieu@univ-amu.fr.

Supplemental material for this article may be found at <http://dx.doi.org/10.1128/AEM.03761-15>.

Copyright © 2016, American Society for Microbiology. All Rights Reserved.

Ustilago maydis whose oxidases play a role in pathogenicity through the production of hydrogen peroxide involved in lesion formation and lesion expansion of the plant cell wall (18, 19).

AAO substrates can include both lignin-derived compounds and aromatic fungal metabolites. Among these compounds, non-phenolic aromatic metabolites seem to be preferred, given the substrate specificity of *Pleurotus eryngii* AAO (PeAAO) (7, 20), but the *Bjerkandera adusta* as well as the *Ustilago maydis* AAOs (BaAAO and UAAO, respectively) efficiently oxidize both non-phenolic and phenolic benzyl alcohols (13, 18). One of the proposed roles for AAO is to provide a continuous supply of H₂O₂ by redox cycling aryl alcohols in collaboration with mycelial dehydrogenases. This process involves two enzymatic activities: an extracellular AAO, which oxidizes aryl alcohols to aldehydes, and an intracellular aryl alcohol NAD(P)⁺ oxidoreductase, which reduces them back to aldehydes (21–23). It has also been postulated that H₂O₂, besides being an oxidizing substrate of ligninolytic peroxidases in white rot decay, could also act as the precursor of highly reactive OH[•], being able to depolymerize lignin (and polysaccharides) (24). Finally, AAOs are also thought to reduce phenoxyl radicals produced by laccase during lignin degradation. This process prevents the polymerization of lignin during its biodegradation by ligninolytic enzymes (25).

The genome of *Pycnoporus cinnabarinus* was recently sequenced to study the enzymatic machinery involved in biomass degradation (26). Among the white rot fungi, *P. cinnabarinus*, which belongs to the *Polyporaceae* family in the phylum of *Basidiomycota*, is known to degrade lignin efficiently and completely (27). Its ligninolytic system features copper- and iron-containing enzymes that are strategic for the targeted transformation of aromatic compounds (28). Of lignin-degrading enzymes, *P. cinnabarinus* is known to secrete a set of native laccases (AA1) at very high levels of up to 1 g · liter⁻¹ (29, 30). Secretome studies in liquid cultures and solid-state fermentation obtained with several substrates highlighted three laccases present under all conditions, demonstrating that these enzymes are efficiently produced by the fungus. Also, four AA3_2 enzymes (scf184803.g17, scf185002.g8, scf184611.g7, and scf184746.g13) were detected in liquid cultures grown on both maltose and birchwood as substrates (26). The enzyme corresponding to scf184803.g17, closely related to glucose oxidase (GOX), was recently characterized and identified as a glucose dehydrogenase, based on its inability to use oxygen as an electron acceptor (31).

In this study, we cloned and heterologously expressed in *Aspergillus niger* the three other AA3_2 enzymes (named aryl-alcohol: quinone oxidoreductases [AAQOs]) produced by *P. cinnabarinus*, termed *P. cinnabarinus* AAQO1 [PcAAQO1], PcAAQO2, and PcAAQO3 for scf185002.g8, scf184611.g7, and scf184746.g13, respectively. Enzymes were fully characterized in terms of physicochemical properties, substrate specificities, reduction of oxidized compounds by *P. cinnabarinus* laccase, and structural properties by homology modeling.

MATERIALS AND METHODS

Chemicals. All reagents were from Sigma-Aldrich.

Strains and culture media. *Escherichia coli* JM109 (Promega, Charbonnières, France) was used for vector propagation. *Aspergillus niger* strain D15#26 (*pyrG* deficient) (32) was used for heterologous expression of the AA3_2-encoding cDNAs. After cotransformation with vectors containing the *pyrG* gene and the expression cassette, transformants of *A.*

TABLE 1 Primers used in this study

Primer name ^a	Sequence
PcAAQO1 for	5'-ATGTCCTTGGCGGCAGCAGC-3'
PcAAQO1 rev	5'-TCAATGCGACAGCGGGATGC-3'
PcAAQO2 for	5'-ATGCGGTGCTTCACGTCAAA-3'
PcAAQO2 rev	5'-TCAGCACCATGCTTCCTTAA-3'
PcAAQO3 for	5'-ATGTAATCTGGCTTCATCGC-3'
PcAAQO3 rev	5'-TCAAGGACACGCTTGCTGTC-3'

^a for, forward; rev, reverse.

niger were grown for selection on solid minimal medium without uridine and containing 70 mM NaNO₃, 7 mM KCl, 11 mM KH₂HPO₄, 2 mM MgSO₄, glucose 1% (wt/vol), and trace elements (1,000× stock; 76 mM ZnSO₄, 178 mM H₃BO₃, 25 mM MnCl₂, 18 mM FeSO₄, 7.1 mM CoCl₂, 6.4 mM CuSO₄, 6.2 mM Na₂MoO₄, 174 mM EDTA). For the screening procedure of the positive transformants, 100 ml of culture medium containing 70 mM NaNO₃, 7 mM KCl, 200 mM Na₂HPO₄, 2 mM MgSO₄, glucose 5% (wt/vol), and trace elements was inoculated with 2 × 10⁶ spores ml⁻¹ in a 250-ml baffled flask. The *P. cinnabarinus* strain BRFM 137 is available at the Centre International de Ressources Microbiennes-Champignons Filamenteux (CIRM-CF [https://www6.inra.fr/cirm_eng/Filamentous-Fungi]).

Cloning and expression of PcAAQO-encoding genes. The open reading frame sequences encoding the three AA3_2 enzymes (Joint Genome Institute [JGI] designations PcAAQO1, PcAAQO2, and PcAAQO3) were amplified on cDNA libraries from *P. cinnabarinus* grown on maltose or birchwood (26) using forward and reverse primers (Table 1), cloned into the pGEM-T Easy Vector System (Promega), and sequenced (GATC Biotech, Constance, Germany) to confirm the exon-intron splicing deduced by bioinformatics. The corresponding sequences were synthesized and codon optimized for *A. niger* (GeneArt), with some modifications. First, the amino acids of the signal peptides, predicted with the program SignalP hosted on the ExPASy Proteomics server (<http://www.expasy.ch>), were replaced by the 24-amino-acid glucoamylase (GLA) preprosequence from *A. niger* (MGFRSLALSLGVCNGLANVISKR). Second, an additional segment encoding a His tag, (CACCAT)₃, was integrated at the C terminus, and two restriction sites (NcoI and HindIII) were added at the 5' and 3' ends of the sequence, respectively, for cloning in the expression vector pAN52.4 (GenBank/EMBL accession number Z32699). In the final expression cassette, the *Aspergillus nidulans* glyceraldehyde-3-phosphate dehydrogenase-encoding gene (*gpdA*) promoter, the 5' untranslated region of the *gpdA* mRNA, and the *A. nidulans trpC* terminator were used to drive the expression of the inserted coding sequences.

Transformation and screening of transformants. For each recombinant protein, cotransformation was carried out as described by Punt and van den Hondel (33) using both the expression vector containing the expression cassette and pAB4-1 (34) containing the *pyrG* selection marker in a 10:1 ratio. Transformants were selected for uridine prototrophy by growth on selective solid minimal medium (without uridine). In order to screen enzyme production in liquid medium, 100 ml of culture minimal medium (adjusted to pH 5.5 with 1 M citric acid) was inoculated with 2 × 10⁶ spores ml⁻¹ in a 250-ml flask. The culture was monitored for 14 days at 30°C in a shaker incubator (130 rpm), and pH was adjusted daily to 5.5 with 1 M citric acid. From these liquid cultures, aliquots (2 ml) were collected daily, and cells were pelleted by centrifugation (20 min at 15,000 × g). The resulting supernatant was concentrated onto microcentrifugal units (Centricon) with a 30-kDa cutoff, and protein production was confirmed by 12% sodium dodecyl sulfate-polyacrylamide gel electrophoresis (SDS-PAGE).

In parallel, aryl alcohol oxidase activity was assayed spectrophotometrically by monitoring the oxidation of 1 mM *p*-methoxybenzyl alcohol to *p*-anisaldehyde at 285 nm (ϵ_{285} , 16.95 mM⁻¹ cm⁻¹) in 100 mM phosphate buffer, pH 6. When no aldehyde production was observed, 200 μM 1,4-benzoquinone (ϵ_{290} , 2.24 mM⁻¹ cm⁻¹) was used as an alternative

electron acceptor. The reactions were followed for 60 s at 30°C in an Uvikon XS spectrophotometer (BioTek Instruments, Colmar, France). Activities are expressed as nkat, the amount of enzyme that oxidizes 1 nanomole of substrate per second.

Purification of the recombinant PcAAQOs. The transformants producing the highest enzyme activity were inoculated under the same conditions as in the screening procedure. One liter of culture per enzyme was harvested after 7 days of growth in a shaking incubator (130 rpm at 30°C), clarified using GF/D, GF/A, and GF/F glass fiber filters (Whatman, Maidstone, United Kingdom), sterile filtered (0.22- μ m-pore-size filter), and concentrated 10-fold by ultrafiltration through a polyether-sulfone membrane with a 10-kDa cutoff (Vivaflow crossflow cassette; Sartorius, Les Ulis, France). The retentates were adjusted to pH 7.8, and the His-tagged recombinant proteins were purified on a Chelating Sepharose Fast Flow column (5-ml Ni Histrap; GE Healthcare, Velizy-Villacoublay, France) equilibrated with five column volumes of binding buffer (50 mM Tris-HCl, pH 7.8, 150 mM NaCl, 10 mM imidazole). After a wash with five column volumes of binding buffer, bound proteins were eluted with five column volumes of 150 mM imidazole in binding buffer at a flow rate of 5 ml min⁻¹ and collected as 1.5-ml fractions. Finally, the fractions of interest were pooled, dialyzed, concentrated by ultrafiltration under nitrogen pressure (rotating membrane with a 10-kDa cutoff; Sartorius), and stored in 100 mM phosphate buffer, pH 6, at -20°C. Protein purification steps were followed by 12% SDS-PAGE. Protein concentrations used in the SDS-PAGE assays were determined spectrophotometrically using molar extinction coefficients at 280 nm of 57,410 M⁻¹ cm⁻¹, 69,900 M⁻¹ cm⁻¹, and 71,640 M⁻¹ cm⁻¹ for PcAAQO1, PcAAQO2, and PcAAQO3, respectively.

N-terminal amino acid sequence determination and enzyme deglycosylation. The N-terminal signal peptides were predicted using SignalP (<http://www.cbs.dtu.dk/services/SignalP/>), and the N-terminal amino acid sequences of the mature proteins were determined according to Edman degradation from a sample electroblotted onto a polyvinylidene difluoride membrane (iBlot; Life Technologies). Analyses were carried out on an Applied Biosystems 470A sequencer by the proteomic platform of the Institut de Microbiologie de la Méditerranée, CNRS, Aix Marseille Université, Marseille, France. Potential N-glycosylation sites were predicted using the CBS NetNGlyc, version 1.0, server (<http://www.cbs.dtu.dk/services/NetNGlyc/>). Recombinant proteins were deglycosylated using peptide-N-glycosidase F (PNGase F) according to the manufacturer's procedure (New England BioLabs, Evry, France). Briefly, 10 μ g of pure enzyme was incubated with 1,000 U of PNGase F for 1 h at 37°C after heat denaturation at 100°C for 10 min. Deglycosylation efficiency was analyzed by 12% SDS-PAGE.

Molar extinction coefficient and spectral characterization. All measurements were performed at 30°C in 100 mM phosphate buffer, at pH 6, using an Uvikon XS spectrophotometer (BioTek Instruments, Colmar, France). The enzyme concentration was determined using the molar absorbance of proteins at 456 nm. These extinction coefficients were determined based on the quantification of free FAD extracted from the protein samples by heat denaturation and using the following equation: $\epsilon_{456} = \epsilon_{\text{FAD}} \times A_{456}/A_{450}$, where A_{456} is the enzyme absorbance at 456 nm, A_{450} is the free-FAD absorbance at 450 nm, and ϵ_{FAD} is the free-FAD extinction coefficient at 450 nm (11,300 M⁻¹ cm⁻¹). Reduction of 24 μ M PcAAQO1 was performed using increasing *p*-anisyl alcohol concentrations of a stock solution of 100 mM, followed by monitoring changes in the protein absorption spectrum.

Substrate specificity and kinetics. All the assays described below were performed using a Uvikon XS spectrophotometer (BioTek Instruments, Colmar, France) for 60 s at 30°C in 100 mM sodium phosphate, pH 6.0 (unless stated otherwise), and reactions were started by the addition of the purified enzymes. Dehydrogenase activity of the recombinant enzymes was assayed spectrophotometrically at the indicated wavelengths using the four electron acceptors (from 1 μ M to 1 mM) 2,6-dichloroindophenol (DCPIP) (ϵ_{520} , 6,800 M⁻¹ cm⁻¹), 1,4-benzoquinone (ϵ_{290} , 2,240 M⁻¹

cm⁻¹), methyl-1,4-benzoquinone (ϵ_{290} , 3,000 M⁻¹ cm⁻¹), and 2,6-dimethyl-1,4-benzoquinone (ϵ_{290} , 2,500 M⁻¹ cm⁻¹) (35) with different alcohol concentrations (from 2.5 μ M to 10 mM) of the following electron donors: veratryl alcohol, *p*-methoxybenzyl alcohol, benzyl alcohol, *m*-methoxybenzyl alcohol, coniferyl alcohol, cinnamyl alcohol, vanillyl alcohol, *p*-hydroxybenzyl alcohol, isovanillyl alcohol, 2-naphthalene methanol, 2,4-hexadien-1-ol, *o*-methoxybenzyl alcohol, 4-chlorobenzyl alcohol, 3-chloro-*p*-methoxybenzyl alcohol, 3-chlorobenzyl alcohol, 3-fluorobenzyl alcohol, and 4-fluorobenzyl alcohol.

Oxidase activity was assayed on the same alcoholic substrates by monitoring H₂O₂ production using a horseradish peroxidase (HRP)-coupled assay with Amplex Red. In the presence of H₂O₂, HRP (6 units/ml) and Amplex Red (60 μ M) form resorufin (ϵ_{563} , 52,000 M⁻¹ cm⁻¹) upon oxidation.

Steady-state parameters were determined using GraphPad software on three replicates of each measurement point. The initial reaction rates at different electron donor or acceptor concentrations were fitted to the Michaelis-Menten equation for one substrate: $v/e = k_{\text{cat}}[S]/(K_m + [S])$, where e is the enzyme concentration, K_m is the Michaelis constant, k_{cat} is the maximal turnover number of the enzyme, and S is the substrate. The catalytic efficiency, k_{cat}/K_m , was determined by fitting the initial rate data to the normalized Michaelis-Menten equation: $v/e = (k_{\text{cat}}/K_m)[S]/(1 + (k_{\text{cat}}/K_m)[S]/k_{\text{cat}})$.

Inhibition of the laccase-catalyzed oxidation of phenolic acids to quinones and phenoxy radicals by PcAAQOs was measured spectrophotometrically using 0.1 mM phenolic acid as the substrate, 0.45 to 3.87 nkat of *P. cinnabarinus* laccase (36), and 2 mM 3-chloro-*p*-methoxybenzyl alcohol for PcAAQO1, 1 mM isovanillyl alcohol for PcAAQO2, and 100 μ M 2,4-hexadien-1-ol for PcAAQO3 as electron donors in 500 μ l of 100 mM sodium acetate buffer, pH 5. The oxidation reactions with or without increasing AAO concentrations were performed at 30°C for 5 min and quantified at the indicated wavelengths.

Temperature and pH stability. To determine the effect of temperature on activities, aliquots of purified recombinant enzymes were incubated at various temperatures ranging from 20°C to 70°C in 100 mM phosphate buffer at pH 6. For the pH profiles, aliquots of purified recombinant enzymes were incubated in 100 mM citrate-phosphate buffer from pH 2.5 to 7.0 and in 100 mM phosphate buffer from pH 7.0 to 11.0. For both experiments, activities were assayed after 10-min incubations using 1 mM 3-chloro-*p*-methoxybenzyl alcohol and 1 mM coniferyl alcohol as electron donor substrates for PcAAQO1 and PcAAQO2, respectively, with 100 μ M 1,4-benzoquinone as acceptor and 200 μ M cinnamyl alcohol as electron donor substrate with 200 μ M DCPIP as acceptor for PcAAQO3. The reactions were followed at the wavelengths indicated above, and measurements were made in triplicate.

Bioinformatic analysis. The open reading frames of 476 representatives of family AA3_2, belonging to the *Polyporales* order, were extracted from the CAZy database (www.cazy.org). In addition, nine sequences for which biochemical data are available were included: glucose oxidases from *Aspergillus niger* (GenBank accession numbers AAA32695.1 and CAC12802.1), *Penicillium chrysogenum* (GenBank AFA42947.1), and *Penicillium amagasakiense* (GenBank P81156); glucose dehydrogenases from *Pycnoporus cinnabarinus* (GenBank KJ934222) and *Glomerella cinogulata* (JF731352); and aryl alcohol oxidases from *Pleurotus eryngii* (GenBank AAC72747.1), *Bjerkandera adusta* (JGI identification number [Bjead1_1]171002), and *Pleurotus pulmonarius* (GenBank AAF31169.1). Finally, the three new recombinant *P. cinnabarinus* AA3_2 enzymes (PcAAQO1, PcAAQO2, and PcAAQO3) identified in the secretomes (26) were also included. Sequence alignments on the resulting 485 sequences were done using ClustalW, and phylogenetic analyses were conducted using the MEGA6 (neighbor-joining) program (37). The pairwise deletion option was active to handle alignment gaps, and the Poisson correction model was used for distance computation. Bootstrap tests were conducted using 1,000 replicates.

TABLE 2 Purification steps for each recombinant enzyme produced in *A. niger* D15 and yield of recombinant PCAAQOs

Enzyme	Purification step	Volume (ml)	Total activity (nkat)	Protein (mg)	Specific activity (nkat/mg)	Activity yield (%)	Purification factor (fold)
PcAAQO1	Culture medium	1,000	20,016	207	97	100	1
	Ultrafiltration	100	16,249	153	106	81	1.1
	Purification	4	12,375	66	188	62	1.94
PcAAQO2	Culture medium	1,000	2,210	113.4	19	100	1
	Ultrafiltration	100	1,610	78.4	21	73	1.1
	Purification	2.8	1,520	68.6	22	69	1.14
PcAAQO3	Culture medium	1,000	2,438	69	35	100	1
	Ultrafiltration	100	2,127	57	37	87	1.1
	Purification	3	1,809	38	48	74	1.35

Multiple alignment analyses of PcAAQO1, PcAAQO2, PcAAQO3, and *P. eryngii* AAO (PDB code 3FIM) were performed using Clustal Omega (<http://www.ebi.ac.uk/Tools/msa/clustalo/>), and the output result was further processed with ESPript, version 3.0 (<http://esprict.ibcp.fr/ESPript/cgi-bin/ESPript.cgi>). The automated protein structure homology modeling program Phyre2 (38) was used to determine the closest protein structure available in the Protein Data Bank (PDB). Using the closest homolog as the template, PeAAO (PDB 3FIM), apo-enzyme modeling was performed. The resulting modeled apo-enzymes were docked with their cofactor FAD (from PDB code 3FIM) using Autodock4 utility scripts (39). The binding cavity, located between the two catalytic histidines and the Rossmann fold, was generated using Autogrid in the AutoDock Tools interface. Dockings were performed by AutoDock, and the results were visualized in Autodock Tools, version 1.5.6. The ligand conformations were assessed manually on lowest binding energy but also according to the *P. eryngii* AAO structure superimposition. Active-site access channels were computed and depicted with the CAVER, version 3.0, PyMOL plug-in (40), and all figures were prepared with PyMOL.

Nucleotide sequence accession numbers. Sequences generated in this study were deposited in GenBank under the following accession numbers: KT327205 for PcAAQO1, KT327206 for PcAAQO2, and KT327207 for PcAAQO3.

RESULTS

Phylogenetic analysis and sequence analysis. A phylogenetic analysis of family AA3_2 representatives obtained from *Polyporales* is presented in Fig. S1 in the supplemental material. A full list of species used and their number of AA3_2-encoding sequences is detailed in Table S1 in the supplemental material. The phylogenetic tree displays eight subgroups (bootstrap values of >70) for which characterized sugar-acting enzymes, glucose oxidase (EC 1.1.3.4) and glucose dehydrogenase (EC 1.1.99.10), were grouped together, whereas characterized AAOs (EC 1.1.3.7) of *P. pulmonarius*, *P. eryngii*, and *B. adusta* were clustered in another subgroup. The PcAAQO1, PcAAQO2, and PcAAQO3 sequences, predicted as AAOs according to blastp, are included in this subgroup. Of these three enzymes, PcAAQO1 exhibited 45.5%, 45%, and 44%, PcAAQO2 had 48.7%, 48.6% and 52%, and PcAAQO3 had 44.5% 44.9%, and 41.3% sequence identity with *P. eryngii*, *P. pulmonarius*, and *B. adusta* aryl alcohol oxidases, respectively. Finally, PcAAQO1 possessed 49% identity with PcAAQO2 and 44% identity with PcAAQO3, while PcAAQO2 possessed 44% identity with PcAAQO3. The six remaining subgroups are genome-derived predictions of unknown functions belonging to the superfamily of GMC oxidoreductases based on blastp searches for which no biochemical data are available.

***A. niger* transformation and screening.** Genome annotation and secretome analysis of *P. cinnabarinus* liquid cultures grown on maltose-, birchwood-, and maize bran-induced media revealed the secretion of four proteins whose genes (PcAAQO1, PcAAQO2, PcAAQO3, and PcGDH) (31) were classified in the superfamily of GMC oxidoreductates, the AA3_2 family (26). In order to produce the other three recombinant enzymes, the coding sequences corresponding to the amino acids of the signal peptides were removed and replaced by the coding sequence of the *A. niger* glucoamylase signal peptide, followed by a KEX2-like cleavage site located in the expression vector pAN52.4. In cotransformation experiments, protoplasts of *A. niger* D15#26 were transformed with both the pAB4-1 plasmid and the expression vector. Transformants were selected for their ability to grow without uridine supplementation. Approximately 75 prototrophic transformants were obtained per microgram of expression vector.

A total of 40 positive clones for each transformation were cultured in standard liquid cultures and checked daily for protein production by SDS-PAGE and for enzymatic activity by spectrophotometric assays. Approximately 20% of the tested transformants exhibited activity in the culture medium. No overexpression was visible on SDS-PAGE, and no AAO activity was detectable in negative controls (transformed by pAB4-1 only). The best-producing clone for each enzyme was selected and cultured in a larger volume for enzyme production and purification.

Purification procedure and study of the biochemical properties. The recombinant enzymes were purified from the culture medium in two successive steps (Table 2). First, 1 liter of culture medium, containing 207 mg, 113.4 mg, and 69 mg of proteins, was concentrated 10-fold by ultrafiltration, with a recovery of 81%, 73%, and 87% for PcAAQO1, PcAAQO2, and PcAAQO3, respectively. Second, 100 ml of the resulting concentrates, containing 153 mg, 78.4 mg, and 57 mg of protein, respectively, was loaded onto a Ni-His trap column and purified to homogeneity, with recoveries of 66 mg, 68.6 mg, and 38 mg for PcAAQO1, PcAAQO2, and PcAAQO3, respectively. The final recovery of the purification ranged from 62% to 74% (Table 2).

The N-terminal sequences obtained for each enzyme were AALTD, LYSDV, and TLFSD for PcAAQO1, PcAAQO2, and PcAAQO3, respectively. Alignment of these N-terminal sequences with the predicted putative sequences confirmed that the 24-amino-acid GLA prepro sequence from *A. niger* was correctly processed.

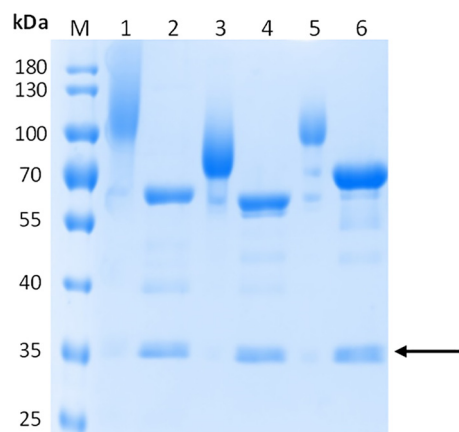


FIG 1 N-glycosylation analysis by SDS-PAGE of purified *PcAAQOs*. Results are shown for glycosylated (lanes 1, 3, and 5, respectively) and deglycosylated (lanes 2, 4, and 6, respectively) *PcAAQO1*, *PcAAQO2*, and *PcAAQO3*. M is the molecular mass marker; the arrow indicates PNGase. Enzymes were stained with Coomassie blue.

Molecular masses for each product were checked on SDS-PAGE gels by electrophoretic mobility of purified protein (Fig. 1). Concerning N-glycosylation, four sites (amino acids 119, 195, 201, and 403 starting from the Met residue) for *PcAAQO1*, two

sites (amino acids 96 and 252 starting from the Met residue) for *PcAAQO2*, and three sites (amino acids 98, 191, and 499 starting from the Met residue) for *PcAAQO3* were predicted following the consensus sequence (Asn-Xaa-Ser/Thr, where Xaa represents an unidentified residue). To confirm the presence of glycosylation (Fig. 1), the purified recombinant enzymes were treated with PNGase, and the resulting proteins showed molecular masses of approximately 65 kDa for *PcAAQO1* and *PcAAQO2*, close to the calculated molecular masses of 63.8 kDa and 62.8 kDa. For *PcAAQO3*, a single band was detected at 70 kDa, suggesting that deglycosylation was not totally efficient since the calculated molecular mass is estimated at 63.4 kDa (Fig. 1).

Spectral properties. The purified enzymes were bright yellow and displayed very similar UV-visible absorption spectra exhibiting the typical bands I and II of the flavin at 385 and 456 nm and a shoulder at 475 nm, indicating that the flavin cofactor was in an oxidized state and correctly incorporated into the protein (Fig. 2). The estimated extinction coefficients at 456 nm (ϵ_{456}) for the purified enzymes were $11,300 \text{ M}^{-1} \text{ cm}^{-1}$, $10,500 \text{ M}^{-1} \text{ cm}^{-1}$, and $13,400 \text{ M}^{-1} \text{ cm}^{-1}$ for *PcAAQO1*, *PcAAQO2*, and *PcAAQO3*, respectively. The A_{280}/A_{456} ratios were found to be 10 for *PcAAQO1*, 12.5 for *PcAAQO2*, and 13 for *PcAAQO3*, indicating that the proteins were mainly in their holoforms.

Addition of increased concentrations of *p*-methoxybenzyl

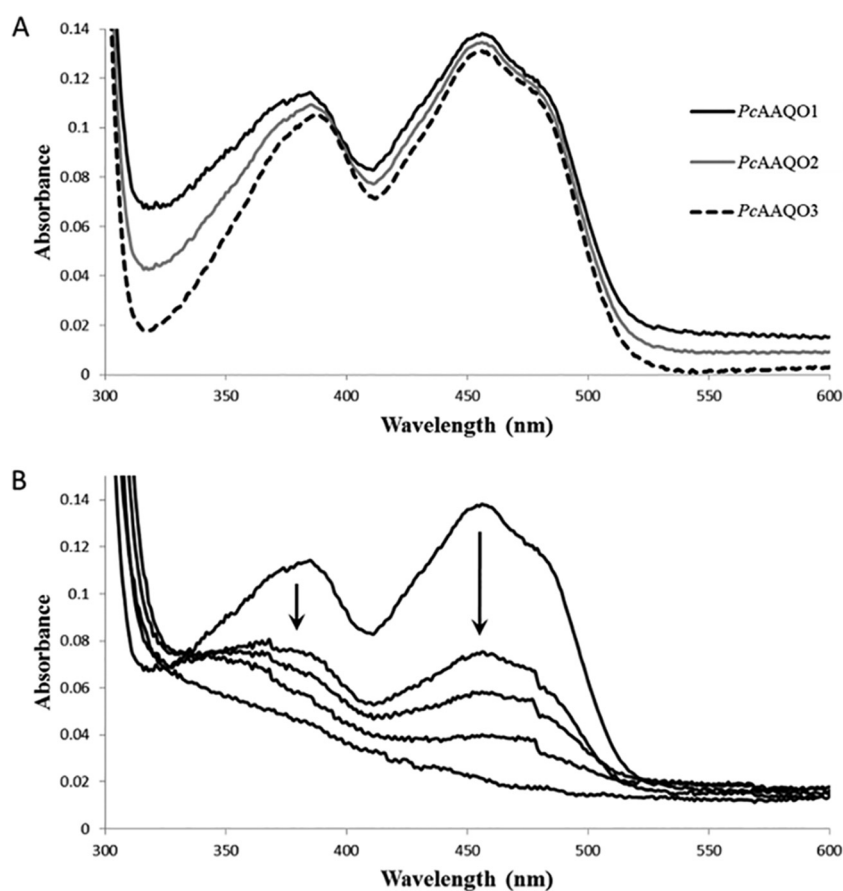
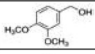
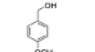
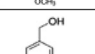
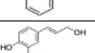
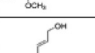
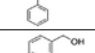
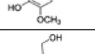
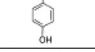
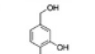
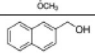
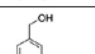
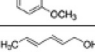
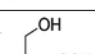
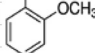
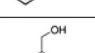
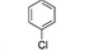
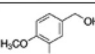


FIG 2 Spectral characterization of recombinant *PcAAQOs*. (A) Visible absorption spectra of purified *PcAAQO1*, *PcAAQO2*, and *PcAAQO3*, as indicated. Spectra were recorded in 100 mM phosphate buffer, pH 6, at 30°C with 24 μM each purified enzyme. (B) Spectral change during reduction of 24 μM *PcAAQO1* by increasing concentrations of *p*-methoxybenzyl alcohol (0, 10, 25, 100, and 250 μM) in 100 mM air-saturated phosphate buffer, pH 6, at 30°C. The arrow indicates the direction of the spectral changes.

TABLE 3 Kinetic parameters for electron donors of *PcAAQOs*^a

Substrate	Structure	<i>PcAAQO1</i>			<i>PcAAQO2</i>			<i>PcAAQO3</i>		
		$K_{m(A)}$ (μ M)	k_{cat} (s^{-1})	$k_{cat}/K_{m(A)}$ ($min^{-1} mM^{-1}$)	$K_{m(A)}$ (μ M)	k_{cat} (s^{-1})	$k_{cat}/K_{m(A)}$ ($min^{-1} mM^{-1}$)	$K_{m(A)}$ (μ M)	k_{cat} (s^{-1})	$k_{cat}/K_{m(A)}$ ($min^{-1} mM^{-1}$)
Veratryl alcohol		766 \pm 34	2.63 \pm 0.03	207 \pm 6	1464 \pm 81	0.65 \pm 0.01	26.6 \pm 1	N.D.	N.D.	N.D.
p-Anisyl alcohol		775 \pm 50	13.1 \pm 0.3	1019 \pm 44	1190 \pm 120	7.47 \pm 0.03	37.9 \pm 2.5	513 \pm 46	1.08 \pm 0.05	127 \pm 7
Benzyl alcohol		N.D.	N.D.	N.D.	5113 \pm 373	14.6 \pm 0.4	2.9 \pm 0.1	3980 \pm 429	1.15 \pm 0.05	17 \pm 2
Coniferyl alcohol		N.D.	N.D.	N.D.	399 \pm 28	0.80 \pm 0.02	121 \pm 6	366 \pm 38	1.05 \pm 0.03	174 \pm 13
Cinnamyl alcohol		391 \pm 45	8.3 \pm 0.4	1280 \pm 83	472 \pm 56	0.8 \pm 0.1	104 \pm 1	275 \pm 16	0.72 \pm 0.02	156 \pm 6
Vanillyl alcohol		N.D.	N.D.	N.D.	N.D.	N.D.	N.D.	1394 \pm 70	1.60 \pm 0.03	69 \pm 3
p-hydroxybenzyl alcohol		N.D.	N.D.	N.D.	1020 \pm 76	0.200 \pm 0.007	11.8 \pm 0.5	1434 \pm 181	0.42 \pm 0.02	17 \pm 2
Isovanillyl alcohol		1233 \pm 72	0.87 \pm 0.02	42 \pm 2	187 \pm 21	0.82 \pm 0.05	266 \pm 16	N.D.	N.D.	N.D.
2-Naphtalene methanol		117 \pm 7	2.10 \pm 0.03	1079 \pm 47	213 \pm 19	1.07 \pm 0.03	301 \pm 19	N.D.	N.D.	N.D.
m-Anisyl alcohol		N.D.	N.D.	N.D.	N.D.	N.D.	N.D.	644 \pm 44	0.28 \pm 0.02	26 \pm 1
2,4-Hexadien-1-ol		750 \pm 37	22.5 \pm 0.3	1805 \pm 66	662 \pm 54	0.44 \pm 0.02	40 \pm 2	88 \pm 7	3.15 \pm 0.08	2151 \pm 127
o-anisyl alcohol (2-Methoxybenzyl alcohol)		N.D.	N.D.	N.D.	N.D.	N.D.	N.D.	N.D.	N.D.	N.D.
4-Chlorobenzyl alcohol		1389 \pm 62	1.08 \pm 0.02	47 \pm 1	941 \pm 68	0.683 \pm 0.017	44 \pm 2	1996 \pm 137	0.25 \pm 0.02	8 \pm 0.5
3-Chloro-p-anisyl alcohol		211 \pm 17	12.8 \pm 0.3	3667 \pm 215	765 \pm 83	0.58 \pm 0.05	46 \pm 1	2244 \pm 213	0.32 \pm 0.02	8.2 \pm 0.5
3-Chlorobenzyl alcohol		3894 \pm 178	1.40 \pm 0.02	22 \pm 1	2182 \pm 200	15.5 \pm 0.1	28 \pm 3	1961 \pm 133	0.78 \pm 0.02	24 \pm 1
3-Fluorobenzyl alcohol		N.D.	N.D.	N.D.	N.D.	N.D.	N.D.	2990 \pm 204	0.95 \pm 0.03	19 \pm 1
4-Fluorobenzyl alcohol		N.D.	N.D.	N.D.	1352 \pm 124	0.70 \pm 0.03	31 \pm 2	993 \pm 82	0.55 \pm 0.02	33 \pm 2

^a The apparent steady-state kinetic constants were determined by varying the alcohol concentration (0.05 to 20 mM) in 100 mM air-saturated phosphate buffer, pH 6, at 30°C in the presence of 100 μ M 1,4-benzoquinone for *PcAAQO1* and *PcAAQO2* and 200 μ M DCPIP for *PcAAQO3* as electron acceptors. The affinity constant for alcohol substrate, $K_{m(A)}$, and turnover number, k_{cat} , were calculated by nonlinear regression using the Michaelis-Menten equation. Data represent means \pm standard deviations ($n = 3$). The detection limit was estimated at 0.5 mIU. ND, not detected.


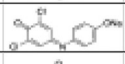
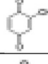
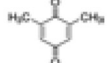
alcohol with *PcAAQO1* resulted in a two-electron reduction of the enzyme, with the disappearance of both peaks. No reoxidation of the reduced FADH₂ cofactor over time was observed (Fig. 2).

Substrate specificities and catalytic properties. The catalytic versatility for each enzyme was determined using a large set of electron donors/acceptors. A wide variety of carbohydrates, including D-glucose, D-galactose, D-mannose, D-xylose, L-arabinose, cellobiose, maltose, and lactose, were also assayed as potential substrates. No activity was detected for carbohydrates and methanol, but primary alcoholic compounds gave activity with the three enzymes (Table 3). The kinetic constants for several

phenolic and nonphenolic benzyl and cinnamyl alcohols and the aliphatic 2,4-hexadien-1-ol were determined and are given in Table 3.

Surprisingly, though predicted as an AAO (see Fig. S1 in the supplemental material), *PcAAQO1* was found to be unable to transfer electrons to molecular oxygen during the oxidative half-reaction. However, it exhibited high efficiency toward other electron acceptors assayed, such as quinones and DCPIP, and so should be considered a strict dehydrogenase. *PcAAQO2* and *PcAAQO3* were able to use oxygen in addition to other electron acceptors; however, they reduced other electron acceptors (quinones or DCPIP) more efficiently than molecular oxygen, and so

TABLE 4 Kinetic parameters for electron acceptors of *PcAAQOs*^a

Acceptor	Structure	<i>PcAAQO1</i>			<i>PcAAQO2</i>			<i>PcAAQO3</i>		
		K _m (μM)	k _{cat} (s ⁻¹)	k _{cat} /K _m (min ⁻¹ mM ⁻¹)	K _m (μM)	k _{cat} (s ⁻¹)	k _{cat} /K _m (min ⁻¹ mM ⁻¹)	K _m (μM)	k _{cat} (s ⁻¹)	k _{cat} /K _m (min ⁻¹ mM ⁻¹)
1,4-Benzoquinone		20 ± 2	17.4 ± 0.4	52596 ± 3960	31 ± 3	1.30 ± 0.03	2534 ± 181	N.D.	N.D.	N.D.
DCIP		27 ± 3	1.16 ± 0.03	2617 ± 216	9 ± 1	0.261 ± 0.003	1764 ± 174	28 ± 3	2.9 ± 0.1	6263 ± 457
Methyl- <i>p</i> -benzoquinone		12 ± 1	7.9 ± 0.1	40063 ± 2755	49 ± 4	0.883 ± 0.017	1087 ± 68	N.D.	N.D.	N.D.
DiMeBQ		267 ± 14	1.92 ± 0.03	431 ± 15	98 ± 9	0.87 ± 0.02	534 ± 39	N.D.	N.D.	N.D.

^a The steady-state kinetic parameters were determined using a fixed saturated concentration of electron donor substrate (1 mM 3-chloro-*p*-anisyl, 1 mM isovanillyl alcohol, and 1 mM 2,4-hexadien-1-ol for *PcAAQO1*, *PcAAQO2*, and *PcAAQO3*, respectively) at 30°C in 100 mM air-saturated phosphate buffer, pH 6, using a concentration range of 0.001 to 1 mM electron acceptor. The affinity constants for the different electron acceptors assayed, $K_{m(Ac)}$, and turnover number, k_{cat} , were calculated by nonlinear regression using the Michaelis-Menten equation. Data represent means ± standard deviations ($n = 3$). The detection limit was estimated at 0.5 mIU. ND, not detected.

should be considered dehydrogenases with some residual oxidase activity (with a ratio of 50:1 of dehydrogenase/oxidase activity).

Table 3 shows the steady-state kinetics toward alcohol electron donors monitored through 1,4-benzoquinone reduction for *PcAAQO1* and *PcAAQO2* and through DCPIP reduction for *PcAAQO3* since no activity was detected using quinones as electron acceptors. Globally, each enzyme displayed distinct catalytic profiles over the compounds studied. *PcAAQO1*, besides possessing the narrowest substrate specificity, was found to be unable to react with benzyl alcohol or phenolic benzyl alcohols, unlike *PcAAQO2* and *PcAAQO3*, which were active against a wider range of substrates, but with differences in affinities. *PcAAQO1* was active against 9 of the 17 compounds studied, showing best catalytic efficiency [$k_{cat}/K_{m(AI)}$ values, where $K_{m(AI)}$ is the affinity constant for an alcohol substrate] with the natural alcohol substrate 3-chloro-*p*-methoxybenzyl, followed by the unsaturated aliphatic alcohol 2,4-hexadien-1-ol and the lignin derivative cinnamyl alcohol. Interestingly, removal of the chloride group for 3-chloro-*p*-methoxybenzyl alcohol (*p*-methoxybenzyl alcohol) affected affinity (K_m values), whereas replacing this group with a methoxy group (veratryl alcohol) or a hydroxyl group (isovanillyl alcohol) affected both affinity and velocity.

Both *PcAAQO2* and *PcAAQO3* displayed broader catalytic spectra (13 of the 17 compounds investigated), with small catalytic efficiencies [$k_{cat}/K_{m(AI)}$ values] due to low catalytic turnovers (k_{cat} values), except for 2,4-hexadien-1-ol for *PcAAQO3*. However, these two enzymes exhibited different substrate specificities. *PcAAQO3* was not active, for instance, on isovanillyl alcohol or 2-naphthalene methanol, which possessed the best affinities toward *PcAAQO2*, whereas it was active on vanillyl alcohol and *m*-methoxybenzyl alcohol, unlike *PcAAQO2* (Table 3).

Regarding natural alcohol substrates of other characterized fungal AAOs, including both lignin-derived compounds and aromatic fungal metabolites, 3-chloro-*p*-methoxybenzyl alcohol, veratryl, and *p*-methoxybenzyl alcohols were poor substrates for *PcAAQO2*; *PcAAQO3* efficiently oxidized only *p*-methoxybenzyl alcohol, while *PcAAQO1* more efficiently oxidized 3-chloro-*p*-methoxybenzyl, *p*-methoxybenzyl, and, to a lesser extent, veratryl alcohols. Among the three enzymes studied, *o*-methoxybenzyl alcohol was not oxidized, and only *PcAAQO3* showed some activity with *m*-fluorobenzyl and *m*-methoxybenzyl alcohols. The three

PcAAQOs efficiently oxidized cinnamyl alcohol, *PcAAQO2* and *PcAAQO3* were active on coniferyl alcohol, and only *PcAAQO3* was active on vanillyl alcohol. The effect of electron-withdrawing substituents on benzyl alcohol was found to be enzyme dependent. *PcAAQO3* oxidized both chloro- and fluoro-substituents in either the *para* or *meta* position, while *PcAAQO1* oxidized only chloro-substituents, and *PcAAQO2* was additionally able to oxidize the *para*-fluoro-substituent (Table 3).

Concerning electron acceptors, for *PcAAQO1*, 1,4-benzoquinone was by far the preferred acceptor, followed by methyl-*p*-benzoquinone, whose turnover was halved. DCPIP exhibited a very high affinity with a low turnover, while dimethyl-benzoquinone displayed a better turnover but with a lower affinity, explaining the difference in catalytic efficiencies for these two compounds (Table 4). For *PcAAQO2*, 1,4-benzoquinone was the compound giving the best catalytic efficiency, followed by DCPIP. Addition of methyl groups decreased catalytic efficiency 2-fold with each addition, affecting both affinity and turnover values. For *PcAAQO3*, only DCPIP was a suitable electron acceptor with a high catalytic efficiency.

Thermal and pH stability. The recombinant enzymes exhibited different stabilities across the pH range assessed (Fig. 3A). *PcAAQO1* was stable at pH 6.0 and retained around 80% activity at pH 4 to 8 and 50% activity at pH 2.5, 3, and 9, and the activity decreased at a pH above 9. *PcAAQO2* was also stable at pH 6.0 and retained 80% activity at acidic pH, i.e., at pH 2.5 to 6; it retained below 40% activity at pH 7.0 and was totally inactive at pH 8.0. *PcAAQO3* retained 80% activity between pH 3 and pH 5, with more stability at pH 4.0, and the activity then decreased to 50% at pH 2.5 or pH 7; at alkaline pH, activity decreased regularly to reach 10% activity at pH 10.

Concerning temperature profiles (Fig. 3B), both *PcAAQO2* and *PcAAQO3* exhibited stability at 60°C after a 10-min incubation, while *PcAAQO1* was more stable at 50°C. *PcAAQO1* was totally inactive at 70°C, while *PcAAQO2* and *PcAAQO3* retained around 40% and 90% activity, respectively, at this temperature. However, both enzymes were totally inactivated at 80°C.

Inhibition of laccase-catalyzed oxidation of phenols and phenoxy radicals. The reduction of the phenoxy lignin precursors generated by *P. cinnabarinus* laccase was studied in an inhibition experiment, given the short lives of these intermediates. For all the

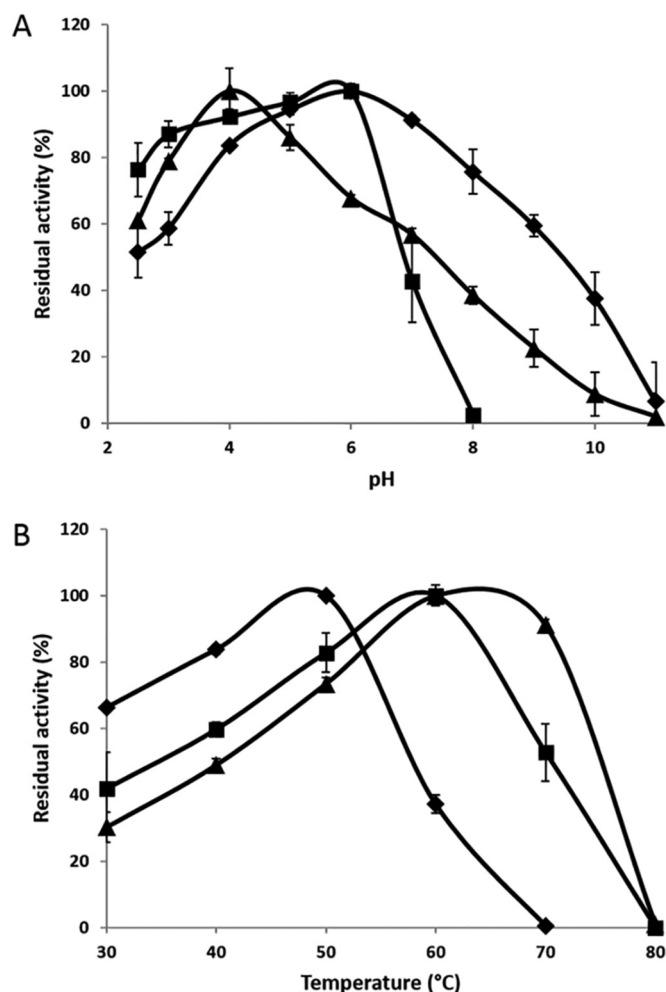


FIG 3 pH (A) and temperature (B) stability of the recombinant *PcAAQO1* (filled diamonds), *PcAAQO2* (filled squares), and *PcAAQO3* (filled triangles) activities. Assays were followed by reduction of 100 μ M 1,4-benzoquinone as an electron acceptor for *PcAAQO1* and *PcAAQO2* and 200 μ M DCPIP for *PcAAQO3* in the presence of 1 mM 3-chloro-*p*-methoxybenzyl alcohol, 1 mM coniferyl alcohol, and 1 mM cinnamyl alcohol as electron donors for *PcAAQO1*, *PcAAQO2*, and *PcAAQO3*, respectively. Data are represented as means \pm standard deviations ($n = 3$). (A) All assays were performed after 10-min incubations at the desired pH in 100 mM citrate-phosphate buffer at 30°C. (B) All assays were performed after 10-min incubations at the desired temperature in 100 mM phosphate buffer, pH 6.

compounds tested, addition of AAO substrate and a concomitantly increased concentration of enzymes drastically reduced both the amount of laccase oxidized products and the rate of formation (Table 5). Inhibition of ferulic acid, coumaric acid, and sinapic acid was not measurable because spectra of either the substrates or the products of *PcAAQO2*, *PcAAQO3*, and laccase overlapped. Even so, for the three enzymes, reduction rates were more marked for caffeic acid than for guaiacol and 2,6-dimethoxyphenol, whose product of oxidation by laccase was the most recalcitrant to reduction by AAOs. In addition to these compounds, *PcAAQO1* was also able to reduce coumaric acid efficiently and, to a lesser extent, ferulic acid.

Molecular modeling and sequence comparison. To gain insight into the structure of *PcAAQOs*, structural modeling was per-

formed using the Phyre2 server (<http://www.sbg.bio.ic.ac.uk/phyre2>). Of the other structurally characterized GMC members, the most structurally similar enzyme to the three *PcAAQOs* was the aryl alcohol oxidase from *Pleurotus eryngii* (PDB code 3FIM), which showed 45%, 47%, and 44% identity to *PcAAQO1*, *PcAAQO2* and *PcAAQO3*, respectively. As a result, homology molecular modeling was performed using this structure as a template. For *PcAAQO1*, 98% of the residues (572) were modeled with >90% accuracy, and 9 residues were modeled *ab initio*; for *PcAAQO2*, 99% of the residues (570) were modeled with >90% accuracy, and 5 residues were modeled *ab initio*; and for *PcAAQO3*, 98% of the residues (583) were modeled with >90% accuracy, and 13 residues were modeled *ab initio*. The stereochemical quality of the predicted models was evaluated through RAMPAGE (41), for which the Ramachandran plot predicted 93%, 96%, and 92.4% of residues lying in the most favored regions for *PcAAQO1*, 184611.g7, and 184746.g13, respectively. The modeled apo-enzymes were then successfully docked with their cofactor FAD and were found to be consistent with the conserved FAD-binding Rossmann fold motif, GXGXXG (where X is any residue) (42) (see Fig. S2, residues 21 to 26, in the supplemental material). Hence, in the vicinity of the flavine ring, both catalytic histidines required for AAO activity are present and in the correct orientations, in front of the flavin *re* side, for catalysis in the three enzymes (Fig. 4). As previously described for *P. eryngii* AAO, a funnel-shaped channel constricted by a bottleneck, involving three aromatic residue side chains (Y92, F397, and F501), connects the active-site cavity to the solvent and provides access for O₂ and reducing substrates to the buried active site (43). Residues involved in the formation of this access channel are drastically different from those in the *P. eryngii* crystal structure (Fig. 4; see also Fig. S2 in the supplemental material). The following numeration was done according to the PDB 3FIM primary sequence: Y92 is replaced by F105 in *PcAAQO1*, by L103 in *PcAAQO2*, and by W104 in *PcAAQO3*; F397 is replaced by L404 in *PcAAQO1*, by A407 in *PcAAQO2*, and by L414 in *PcAAQO3*. For *PcAAQO2*, the structure-based alignment rendered by ESPRIT indicated that F411 was aligned with F397, but based on structural analysis, L414 was chosen instead. F501, the most crucial residue for enzyme reoxidation, was replaced by R514 in *PcAAQO1* and by W510/W517 in *PcAAQO2* and *PcAAQO3*. In addition, to assess O₂ diffusion from the solvent to the active site in our modeled holoenzymes, access channels were computed and depicted with CAVER, version 3.0, software (Fig. 5). These access channels are wider than the one of *P. eryngii* AAO, and no comparable constriction is observed, which might explain the absence of or only low reactivity with oxygen as an electron acceptor during the oxidative half-reaction.

DISCUSSION

This work presents the study of AAO secreted from the white rot fungus *P. cinnabarinus*. The heterologous production and characterization of these enzymes are useful in lending additional biochemical insights into the AA3_2 members and their role during lignolysis. Members of the AA3_2 group belong to the GMC oxidoreductase family represented by a wide variety of catalytically diverse enzymes of both prokaryotic and eukaryotic origins, including aryl alcohol oxidases (1). By analyzing the phylogenetic distribution of *PcAAQO1*, *PcAAQO2*, and *PcAAQO3* among the AA3_2 enzymes of the *Polyporales* order, we demonstrate that

TABLE 5 Reduction of laccase-catalyzed oxidative phenoxyl radical formation after addition of *Pc*AAQOs^a

Substrate	Structure	λ (nm)	laccase (nkat)	rate reduction by <i>Pc</i> AAQO1					rate reduction by <i>Pc</i> AAQO2 (%)					rate reduction by <i>Pc</i> AAQO3 (%)				
				1.25 nkat	2.5 nkat	5 nkat	7.5 nkat	10 nkat	1.25 nkat	2.5 nkat	5 nkat	7.5 nkat	10 nkat	1.25 nkat	2.5 nkat	5 nkat	7.5 nkat	10 nkat
Ferulic acid		285	1	14.3	18.8	23.5	25.8	29.5	N.M.	N.M.	N.M.	N.M.	N.M.	N.M.	N.M.	N.M.	N.M.	N.M.
Coumaric acid		285	3.87	11	24	42.7	64.5	100	N.M.	N.M.	N.M.	N.M.	N.M.	N.M.	N.M.	N.M.	N.M.	N.M.
Sinapic acid		305	0.45	0	0	0	0	0	N.M.	N.M.	N.M.	N.M.	N.M.	N.M.	N.M.	N.M.	N.M.	N.M.
Caffeic acid		315	1	47.3	75.8	100	100	100	33.5	63.1	74.4	85.6	100	92.1	100	100	100	100
Guaiacol		465	3.87	27	49	76.2	82.5	100	28.2	37.5	41.3	55.67	86.8	44.31	51.3	56	77.5	91.3
2,6-Dimethoxyphenol		469	0.45	3.1	5.7	13.6	17.6	20.6	1.3	17	31.5	38.2	45.5	6.7	12.2	15.7	23.1	35.7

^a The laccase-catalyzed oxidation reactions and their inhibition by increasing *Pc*AAQO concentrations were followed spectrophotometrically at the indicated wavelength for each compound using a fixed saturated concentration of electron donor substrate (2 mM 3-chloro-*p*-anisyl, 1 mM isovanillyl alcohol, and 100 μ M 2,4-hexadien-1-ol for *Pc*AAQO1, *Pc*AAQO2, and *Pc*AAQO3, respectively) at 30°C in 100 mM sodium acetate buffer, pH 5.

they belong to the same group as other biochemically characterized AAOs (see Fig. S1 in the supplemental material). Based on blastp similarities and phylogenetic analysis, the corresponding enzymes were predicted as putative aryl alcohol oxidases.

The *Pc*AAQO1-, *Pc*AAQO2-, and *Pc*AAQO3-encoding genes are demonstrated to be functional as the corresponding enzymes were identified in secretomes grown on maltose and birchwood media (26). So far, only a few AAOs have been biochemically characterized (7, 9, 13, 18); the most extensively studied one is from *P. eryngii*, whose crystal structure, the only one available for this class of enzymes, was resolved in 2009 at a 2.4-Å resolution (44). *A. niger* has been used in previous work to produce fungal oxidases (laccases) at relatively high yield (45, 46), and flavo-enzymes, such as cellobiose dehydrogenase from *Coprinopsis cinerea* (47) and glucose dehydrogenase from *P. cinnabarinus* (31), have also been used. Under our conditions, *A. niger* gave a secretion yield of 69 to 207 mg liter⁻¹ of recombinant enzymes in nonoptimized 7-day cultures. After purification in two steps, ultrafiltration, and affinity chromatography, 38 to 69 mg of pure enzymes was recovered from 1 liter of culture medium (Table 2).

The purified enzymes, deglycosylated using an *N*-glycosidase, had molecular masses of approximately 65 kDa (predicted molecular masses of 64 kDa and 62 kDa for *Pc*AAQO1 and *Pc*AAQO2, respectively), indicating that deglycosylation was probably complete and that glycosylation was N-linked for these two enzymes. In the case of *Pc*AAQO3, deglycosylation was not totally efficient, with the molecular mass, estimated at 63.4 kDa, being lower than the band detected at 70 kDa after *N*-glycosidase treatment (Fig. 1). These glycosylations accounted for approximately 10% for *Pc*AAQO2 and 42% for *Pc*AAQO1 and *Pc*AAQO3 of the total mass of the proteins. The last value contrasts with that of *P. eryngii* AAO produced in *A. nidulans*, for which 14% of N-glycosylations were suggested (48). However, these high values were probably overestimated by SDS-PAGE owing to the presence of band smears on the gel.

The three recombinant proteins were characterized by their main biochemical and physicochemical properties in order to study their mechanisms of action and compare them with other

experimentally characterized AAOs. Our recombinant AAOs possessed the highest temperature stability after 10-min incubations at 50°C for *Pc*AAQO1 and at 60°C for *Pc*AAQO2 and *Pc*AAQO3, but no information on temperature stability is available for other fungal AAOs. pH-dependent stability was optimal at pH 6 for *Pc*AAQO1 and *Pc*AAQO2 and at pH 4 for *Pc*AAQO3. *Pc*AAQO1 exhibited broad pH stability, with more than 80% activity on 3-chloro-*p*-anisyl in the range pH 4 to 7, while *Pc*AAQO2 showed a more acidic pH range of 2.5 to 6 and drastically lost activity at pH 7. Finally, *Pc*AAQO3 exhibited the narrowest stability, at pH 3 to 5. These values are in the range of those of other fungal AAOs, which also possessed optimal pH stability at values around 6, with no significant changes in acidic conditions at pH 4 to 7 (13, 18, 20).

Considering the various electron donors assayed (aryl alcohols, methanol, and carbohydrates), we observed that at least one double bond conjugated with a primary alcohol is necessary for substrate recognition by *Pc*AAQOs. Concerning substrate specificity, *Pc*AAQO1 possesses a catalytic spectrum similar to that of *Pe*AAO, with the exception of benzyl alcohol and its fluoro-substituted derivatives, and, unlike *Pc*AAQO3, is inactive on phenolic benzyl alcohols (20). *Pc*AAQO3 exhibits a catalytic spectrum comparable to that of *Ba*AAO or *Um*AAO, except for veratryl and isovanillyl alcohols (13, 18). These compounds are among the typical substrates of vanillyl-alcohol oxidase, another flavoenzyme from a different family, which requires the presence of the hydroxyl group at the *p*-position on the benzene ring to oxidize alcohols to the corresponding aldehydes (49). *Pc*AAQO3 presented similar behavior, oxidizing vanillyl alcohol and *p*-hydroxybenzyl alcohol (hydroxyl group at the *p*-position), but not isovanillyl alcohol (hydroxyl group at the *m*-position), while *Pc*AAQO1 presented the opposite effect: it was active on isovanillyl alcohol but not on vanillyl alcohol or *p*-hydroxybenzyl alcohol (Table 3). *Pc*AAQO2 displays a catalytic spectrum between the spectra of *Pc*AAQO1 and *Pc*AAQO3, being active on two of the three phenolic benzyl alcohols assayed (coniferyl and *p*-hydroxybenzyl alcohols). It also oxidized isovanillyl alcohol more efficiently than *Pc*AAQO1 due to a low affinity constant, with both enzymes displaying the same

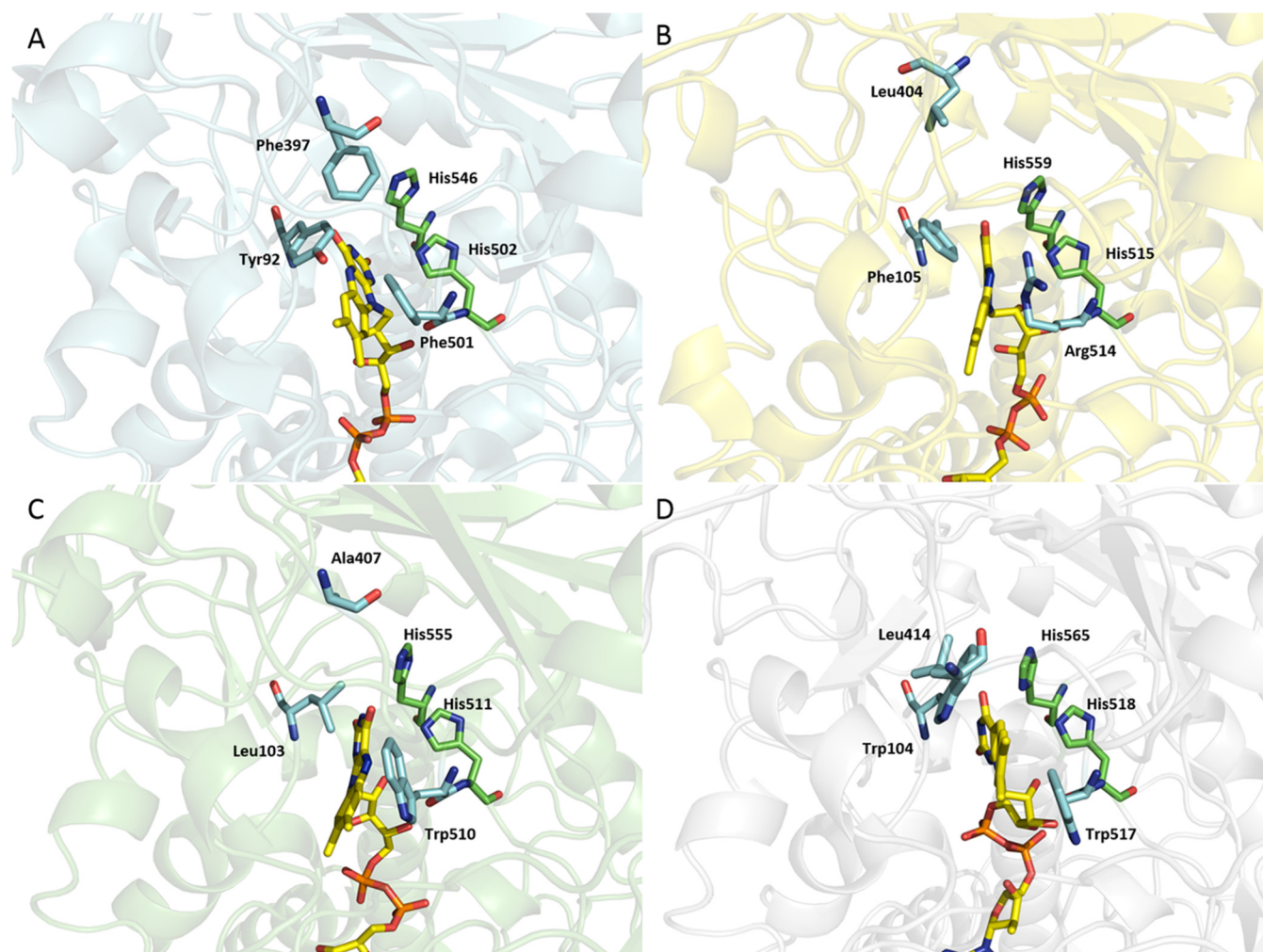


FIG 4 Comparison of the active sites for *P. eryngii* AAO (PDB code 3FIM) (A), PcAAQO1 (B), PcAAQO2 (C), and PcAAQO3 (D) docked with FAD. Catalytic histidines are shown in green, residues involved in the substrate access channel formation are shown in light blue, and the FAD cofactor molecule is shown in yellow.

turnover rates for this compound. Taken together, these results demonstrate the importance of the hydroxyl substituent position for AAO activities as observed for *PeAAO* (20). In addition, the presence of additional conjugated double bonds enhanced PcAAQO3 selectivity since cinnamyl alcohol, cinnamyl alcohol, and the aliphatic 2,4-hexadien-1-ol were the compounds possessing the strongest affinities.

Among the natural substrates assayed (lignin derivatives or fungal metabolite), 3-chloro-*p*-anisyl, isovanillyl, and cinnamyl alcohols presented the strongest affinity toward PcAAQO1, PcAAQO2, and PcAAQO3, with K_m values of 211 μ M, 187 μ M, and 275 μ M, respectively (Table 3). The values obtained for 3-chloro-*p*-methoxybenzyl alcohol with PcAAQO1 were 15-fold those of *P. eryngii* AAO (14 μ M) and 4-fold those of *B. adusta* AAO (49 μ M). Isovanillyl alcohol K_m values were higher for *P. eryngii* AAO (831 μ M) and *B. adusta* AAO (1113 μ M), while for cinnamyl alcohol, K_m values were higher for *P. eryngii* AAO (708 μ M) and lower for *B. adusta* (73 μ M) and *U. maydis* (35 μ M) AAOs (13, 20). These three compounds were not tested for *Pleurotus pulmonarius* AAO (9) while 3-chloro-*p*-methoxybenzyl and isovanillyl alcohols were not tested for *U. maydis* AAO (18).

Though predicted as AAOs, PcAAQOs demonstrated no or very low reactivity with molecular oxygen as an electron acceptor (data not shown). In order to obtain further insights into the enzyme mechanism, a structure-based alignment of PcAAQO1, PcAAQO2, and PcAAQO3 against *PeAAO*, together with molecular modeling using *PeAAO* (PDB code 3FIM) as a template, was undertaken. As a general point, we observed that the catalytic residues of *PeAAO*, H502 and H546, were conserved among PcAAQOs, as well as the residues involved in the Rossmann fold responsible for FAD binding (see Fig. S2 in the supplemental material). However, residues involved in the formation of the substrate access channel were different from those in *PeAAO* (Fig. 5; see also Fig. S2). These differences in the substrate access channel leading to the active-site cavity could explain the residual activity (PcAAQO2 and PcAAQO3), or the absence (PcAAQO1) of reactivity, with oxygen as an electron acceptor. In *PeAAO*, a narrow substrate access channel constricted by three aromatic amino acids is responsible for guiding and positioning the oxygen from the solvent to the active site (Fig. 5A). Also, Phe501 adjacent to the catalytic His502 was demonstrated to be crucial for O_2 affinity and turnover. By removing the aromatic side chain of this

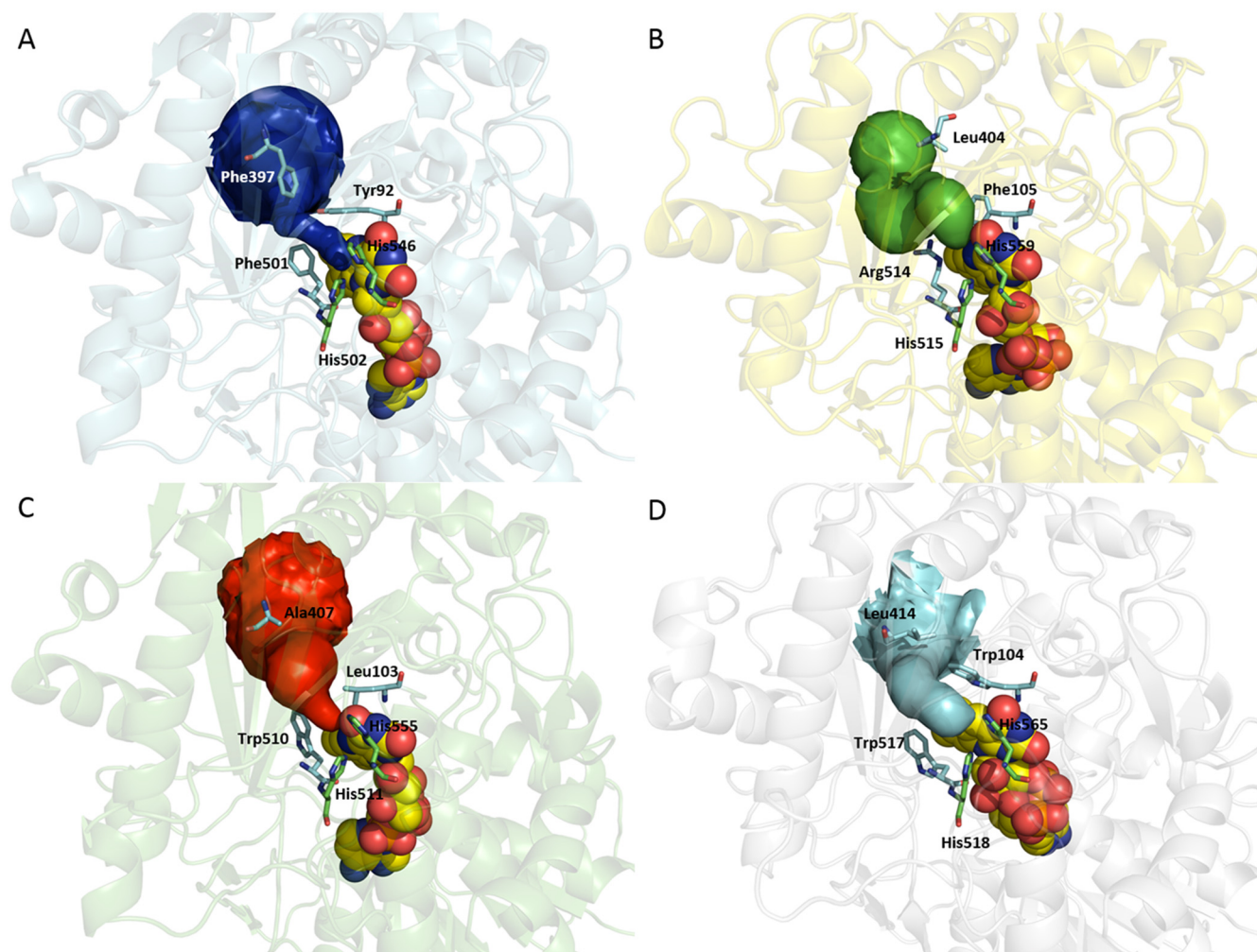


FIG 5 Comparison of the channels connecting the active-site cavity to solvent in *P. eryngii* AAO (PDB code 3FIM) (A), PcAAQO1 (B), PcAAQO2 (C), and PcAAQO3 (D). The active-site access channels were depicted by CAVER (40). FAD is shown as Corey-Pauling-Koltun (CPK)-colored van der Waals spheres, catalytic histidines are shown in green, and residues involved in the substrate access channel formation are shown in light blue.

residue (F501A), a 71-fold decrease in the catalytic efficiency and a 27-fold decrease in the affinity for oxygen were observed (43). In contrast, increasing the steric hindrance of this residue (F501W) and thus narrowing the access channel increased catalytic efficiency 2-fold and affinity 3-fold (43). As shown in Fig. 5, the PcAAQO residues involved in the substrate access channel are not all aromatics, leading to a wider access channel and thus explaining the absence of reactivity with oxygen as an electron acceptor for these enzymes. In future work, genetically changing the corresponding amino acids in PcAAQOs to obtain new data on the relationship between steric hindrance, the substrate access channel, and oxygen reactivity could thus be considered.

The biological function of AAO in *P. eryngii* is to participate in H_2O_2 supply for peroxidases by redox cycling aryl alcohols between extracellular AAO and intracellular aryl alcohol dehydrogenase (21). Despite their similarity to other fungal AAOs, the catalytic efficiency of PcAAQOs toward oxygen raises the question of these enzymes as H_2O_2 suppliers for peroxidases; the ability of PcAAQOs to reduce phenoxy radicals generated by laccase (Table 5) coupled to their lack of, or low, reactivity with oxygen could indicate another biological role in *P. cinnabarinus*. Secretome

studies of this fungus demonstrate that in liquid cultures and solid-state fermentation three laccases were detected, with one as the major enzyme. In contrast, peroxidases were detected only in solid-state fermentation (one LiP and one manganese peroxidase [MnP]), with low peptide numbers compared with those of laccase. These results indicate a major role for laccase during biomass decomposition. Depending on substrates and culture conditions, PcAAQO1, PcAAQO2, and PcAAQO3 were also detected with higher peptide numbers than peroxidases (26). The synergy between laccase and AAO during lignin degradation has already been observed for another white rot fungus, *Pleurotus ostreatus* (25). Hence, in *P. cinnabarinus*, the cosecretion of PcAAQOs with laccase and their ability to use lignin-derived aryl alcohols (Table 3), as well as reducing phenoxy radicals generated by laccases (Table 5), indicate a similar role for PcAAQOs during biomass degradation in preventing the polymerization of lignin during its oxidation by laccase, instead of supplying H_2O_2 to peroxidases. Alternatively, the ability of these enzymes to efficiently reduce different quinones, which are intermediates in the degradation of aromatic compounds by wood-rotting fungi (50), could indicate another potential biological role. During lignin degradation these

compounds either could be reduced to hydroquinones by PcAAQOs, which are then further metabolized intracellularly (51, 52), or enter an extracellular redox cycle that contributes to the generation of reactive oxygen species (ROS) for nonenzymatic attack of lignocellulose (53).

ACKNOWLEDGMENTS

We thank Pascal Mansuelle and Régine Lebrun from the proteomics platform of the Institut de Microbiologie de la Méditerranée, CNRS-AMU, Marseille, France, for protein N-terminal sequencing. We also thank David Navarro from the UMR 1163 Biotechnologie des Champignons Filamenteux for the high performance liquid chromatography analysis of the enzymatic reactions. Finally, we thank Bernard Henrissat from the UMR Architecture et Fonction des Macromolécules Biologiques for providing the AA3_2 sequences from the CAZy database for bioinformatic analyses.

FUNDING INFORMATION

European Commission (EC) provided funding to Yann Mathieu, François Piumi, Richard Valli, Juan Carro Aramburu, Patricia Ferreira, Craig B. Faulds, and Eric Record under grant number KBBE-2013-7-613549.

REFERENCES

- Levasseur A, Drula E, Lombard V, Coutinho PM, Henrissat B. 2013. Expansion of the enzymatic repertoire of the CAZy database to integrate auxiliary redox enzymes. *Biotechnol Biofuels* 6:41. <http://dx.doi.org/10.1186/1754-6834-6-41>.
- Levasseur A, Piumi F, Coutinho PM, Rancurel C, Asther M, Delattre M, Henrissat B, Pontarotti P, Asther M, Record E. 2008. FOLY: an integrated database for the classification and functional annotation of fungal oxidoreductases potentially involved in the degradation of lignin and related aromatic compounds. *Fungal Genet Biol* 45:638–645. <http://dx.doi.org/10.1016/j.fgb.2008.01.004>.
- Ruiz-Dueñas FJ, Martínez AT. 2009. Microbial degradation of lignin: how a bulky recalcitrant polymer is efficiently recycled in nature and how we can take advantage of this. *Microb Biotechnol* 2:164–177. <http://dx.doi.org/10.1111/j.1751-7915.2008.00078.x>.
- Cavener DR. 1992. GMC oxidoreductases: a newly defined family of homologous proteins with diverse catalytic activities. *J Mol Biol* 223:811–814. [http://dx.doi.org/10.1016/0022-2836\(92\)90992-S](http://dx.doi.org/10.1016/0022-2836(92)90992-S).
- Farmer V, Henderson ME, Russell J. 1960. Aromatic-alcohol-oxidase activity in the growth medium of *Polystictus versicolor*. *Biochem J* 74:257. <http://dx.doi.org/10.1042/bj0740257>.
- Bourbonnais R, Paice MG. 1988. Veratryl alcohol oxidases from the lignin-degrading basidiomycete *Pleurotus sajor-caju*. *Biochem J* 255:445–450. <http://dx.doi.org/10.1042/bj2550445>.
- Guillén F, Martínez AT, Martínez MJ. 1992. Substrate specificity and properties of the aryl-alcohol oxidase from the ligninolytic fungus *Pleurotus eryngii*. *Eur J Biochem* 209:603–611. <http://dx.doi.org/10.1111/j.1432-1033.1992.tb17326.x>.
- Sannia G, Limongi P, Cocca E, Buonocore F, Nitti G, Giardina P. 1991. Purification and characterization of a veratryl alcohol oxidase enzyme from the lignin degrading basidiomycete *Pleurotus ostreatus*. *Biochim Biophys Acta* 1073:114–119. [http://dx.doi.org/10.1016/0304-4165\(91\)90190-R](http://dx.doi.org/10.1016/0304-4165(91)90190-R).
- Varela E, Böckle B, Romero A, Martínez AT, Martínez MJ. 2000. Biochemical characterization, cDNA cloning and protein crystallization of aryl-alcohol oxidase from *Pleurotus pulmonarius*. *Biochim Biophys Acta* 1476:129–138. [http://dx.doi.org/10.1016/S0167-4838\(99\)00227-7](http://dx.doi.org/10.1016/S0167-4838(99)00227-7).
- Iwahara S, Nishihara T, Jomori T, Kuwahara M, Higuchi T. 1980. Enzymic oxidation of α,β -unsaturated alcohols in the side chains of lignin-related aromatic compounds. *J Ferment Technol* 58:183–188.
- Waldner R, Leisola MS, Fiechter A. 1988. Comparison of ligninolytic activities of selected white-rot fungi. *Appl Microbiol Biotechnol* 29:400–407. <http://dx.doi.org/10.1007/BF00265826>.
- Kimura Y, Asada Y, Kuwahara M. 1990. Screening of basidiomycetes for lignin peroxidase genes using a DNA probe. *Appl Microbiol Biotechnol* 32:436–442. <http://dx.doi.org/10.1007/BF00903779>.
- Romero E, Ferreira P, Martínez AT, Martínez MJ. 2009. New oxidase from *Bjerkandera arthroconidial* anamorph that oxidizes both phenolic and nonphenolic benzyl alcohols. *Biochim Biophys Acta* 1794:689–697. <http://dx.doi.org/10.1016/j.bbapap.2008.11.013>.
- Goetghebeur M, Brun S, Galzy P, Nicolas M. 1993. Benzyl alcohol oxidase and laccase synthesis in *Botrytis cinerea*. *Biosci Biotechnol Biochem* 57:1380–1381. <http://dx.doi.org/10.1271/bbb.57.1380>.
- Muheim A, Leisola MS, Schoemaker HE. 1990. Aryl-alcohol oxidase and lignin peroxidase from the white-rot fungus *Bjerkandera adusta*. *J Biotechnol* 13:159–167. [http://dx.doi.org/10.1016/0168-1656\(90\)90101-G](http://dx.doi.org/10.1016/0168-1656(90)90101-G).
- Camarero S, Bockle B, Martínez MJ, Martínez AT. 1996. Manganese-mediated lignin degradation by *Pleurotus pulmonarius*. *Appl Environ Microbiol* 62:1070–1072.
- Barrasa J, Gutiérrez A, Escaso V, Guillén F, Martínez M, Martínez A. 1998. Electron and fluorescence microscopy of extracellular glucan and aryl-alcohol oxidase during wheat-straw degradation by *Pleurotus eryngii*. *Appl Environ Microbiol* 64:325–332.
- Couturier M, Mathieu Y, Li A, Navarro D, Drula E, Haon M, Grisel S, Ludwig R, Berrin J-G. 2016. Characterization of a new aryl-alcohol oxidase secreted by the phytopathogenic fungus *Ustilago maydis*. *Appl Microbiol Biotechnol* 100:697–706. <http://dx.doi.org/10.1007/s00253-015-7021-3>.
- Leuthner B, Aichinger C, Oehmen E, Koopmann E, Müller O, Müller P, Kahmann R, Bölker M, Schreier PH. 2005. A H₂O₂-producing glyoxal oxidase is required for filamentous growth and pathogenicity in *Ustilago maydis*. *Mol Genet Genomics* 272:639–650. <http://dx.doi.org/10.1007/s00438-004-1085-6>.
- Ferreira P, Medina M, Guillén F, Martínez M, Van Berkel W, Martínez A. 2005. Spectral and catalytic properties of aryl-alcohol oxidase, a fungal flavoenzyme acting on polyunsaturated alcohols. *Biochem J* 389:731–738. <http://dx.doi.org/10.1042/BJ20041903>.
- Guillén F, Martínez A, Martínez M, Evans C. 1994. Hydrogen-peroxide-producing system of *Pleurotus eryngii* involving the extracellular enzyme aryl-alcohol oxidase. *Appl Microbiol Biotechnol* 41:465–470. <http://dx.doi.org/10.1007/BF00939037>.
- Gutiérrez A, Caramelo L, Prieto A, Martínez MJ, Martínez AT. 1994. Anisaldehyde production and aryl-alcohol oxidase and dehydrogenase activities in ligninolytic fungi of the genus *Pleurotus*. *Appl Environ Microbiol* 60:1783–1788.
- Guillén F, Evans CS. 1994. Anisaldehyde and veratraldehyde acting as redox cycling agents for H₂O₂ production by *Pleurotus eryngii*. *Appl Environ Microbiol* 60:2811–2817.
- Guillén F, Gómez-Toribio V, Martínez MJ, Martínez AT. 2000. Production of hydroxyl radical by the synergistic action of fungal laccase and aryl alcohol oxidase. *Arch Biochem Biophys* 383:142–147. <http://dx.doi.org/10.1006/abbi.2000.2053>.
- Marzullo L, Cannio R, Giardina P, Santini MT, Sannia G. 1995. Veratryl alcohol oxidase from *Pleurotus ostreatus* participates in lignin biodegradation and prevents polymerization of laccase-oxidized substrates. *J Biol Chem* 270:3823–3827. <http://dx.doi.org/10.1074/jbc.270.8.3823>.
- Levasseur A, Lomascolo A, Chabrol O, Ruiz-Duenas FJ, Boukhris-Uzan E, Piumi F, Kues U, Ram AF, Murat C, Haon M, Benoit I, Arfi Y, Chevret D, Drula E, Kwon MJ, Gouret P, Lesage-Meessen L, Lombard V, Mariette J, Noirot C, Park J, Patyshakuliyeva A, Sigoillot JC, Wiebenga A, Wosten HA, Martin F, Coutinho PM, de Vries RP, Martínez AT, Klopp C, Pontarotti P, Henrissat B, Record E. 2014. The genome of the white-rot fungus *Pycnoporus cinnabarinus*: a basidiomycete model with a versatile arsenal for lignocellulosic biomass breakdown. *BMC Genomics* 15:486. <http://dx.doi.org/10.1186/1471-2164-15-486>.
- Lomascolo A, Uzan-Boukhris E, Herpoël-Gimbart I, Sigoillot J-C, Lesage-Meessen L. 2011. Peculiarities of *Pycnoporus* species for applications in biotechnology. *Appl Microbiol Biotechnol* 92:1129–1149. <http://dx.doi.org/10.1007/s00253-011-3596-5>.
- Lomascolo A, Stentelaire C, Asther M, Lesage-Meessen L. 1999. Basidiomycetes as new biotechnological tools to generate natural aromatic flavours for the food industry. *Trends Biotechnol* 17:282–289. [http://dx.doi.org/10.1016/S0167-7799\(99\)01313-X](http://dx.doi.org/10.1016/S0167-7799(99)01313-X).
- Eggert C, Temp U, Eriksson K-E. 1996. The ligninolytic system of the white rot fungus *Pycnoporus cinnabarinus*: purification and characterization of the laccase. *Appl Environ Microbiol* 62:1151–1158.
- Lomascolo A, Record E, Herpoël-Gimbart I, Delattre M, Robert J, Georis J, Dauvin T, Sigoillot JC, Asther M. 2003. Overproduction of laccase by a monokaryotic strain of *Pycnoporus cinnabarinus* using ethanol as inducer. *J Appl Microbiol* 94:618–624. <http://dx.doi.org/10.1046/j.1365-2672.2003.01879.x>.
- Piumi F, Levasseur A, Navarro D, Zhou S, Mathieu Y, Ropartz D, Ludwig R, Faulds CB, Record E. 2014. A novel glucose dehydrogenase

- from the white-rot fungus *Pycnoporus cinnabarinus*: production in *Aspergillus niger* and physicochemical characterization of the recombinant enzyme. *Appl Microbiol Biotechnol* 98:10105–10118. <http://dx.doi.org/10.1007/s00253-014-5891-4>.
32. Gordon CL, Khalaj V, Ram AF, Archer DB, Brookman JL, Trinci AP, Jeenes DJ, Doonan JH, Wells B, Punt PJ, van den Hondel CA, Robson GD. 2000. Glucoamylase: green fluorescent protein fusions to monitor protein secretion in *Aspergillus niger*. *Microbiology* 146:415–426. <http://dx.doi.org/10.1099/00221287-146-2-415>.
 33. Punt PJ, van den Hondel CA. 1992. Transformation of filamentous fungi based on hygromycin B and phleomycin resistance markers. *Methods Enzymol* 216:447–457. [http://dx.doi.org/10.1016/0076-6879\(92\)16041-H](http://dx.doi.org/10.1016/0076-6879(92)16041-H).
 34. van Hartingsveldt W, Mattern IE, van Zeijl CM, Pouwels PH, van den Hondel CA. 1987. Development of a homologous transformation system for *Aspergillus niger* based on the *pyrG* gene. *Mol Gen Genet* 206:71–75. <http://dx.doi.org/10.1007/BF00326538>.
 35. Sygmond C, Klausberger M, Felice AK, Ludwig R. 2011. Reduction of quinones and phenoxy radicals by extracellular glucose dehydrogenase from *Glomerella cingulata* suggests a role in plant pathogenicity. *Microbiology* 157:3203–3212. <http://dx.doi.org/10.1099/mic.0.051904-0>.
 36. Sigoillot C, Record E, Belle V, Robert JL, Levasseur A, Punt PJ, van den Hondel CA, Fournel A, Sigoillot JC, Asther M. 2004. Natural and recombinant fungal laccases for paper pulp bleaching. *Appl Microbiol Biotechnol* 64:346–352. <http://dx.doi.org/10.1007/s00253-003-1468-3>.
 37. Tamura K, Stecher G, Peterson D, Filipski A, Kumar S. 2013. MEGA6: Molecular Evolutionary Genetics Analysis version 6.0. *Mol Biol Evol* 30:2725–2729. <http://dx.doi.org/10.1093/molbev/mst197>.
 38. Kelley LA, Mezulis S, Yates CM, Wass MN, Sternberg MJE. 2015. The Phyre2 web portal for protein modeling, prediction and analysis. *Nat Protoc* 10:845–858. <http://dx.doi.org/10.1038/nprot.2015.053>.
 39. Morris GM, Huey R, Lindstrom W, Sanner MF, Belew RK, Goodsell DS, Olson AJ. 2009. AutoDock4 and AutoDockTools4: automated docking with selective receptor flexibility. *J Comput Chem* 30:2785–2791. <http://dx.doi.org/10.1002/jcc.21256>.
 40. Chovancova E, Pavelka A, Benes P, Strnad O, Brezovsky J, Kozlikova B, Gora A, Sustr V, Klvana M, Medek P, Biedermannova L, Sochor J, Damborsky J. 2012. CAVER 3.0: a tool for the analysis of transport pathways in dynamic protein structures. *PLoS Comput Biol* 8:e1002708. <http://dx.doi.org/10.1371/journal.pcbi.1002708>.
 41. Lovell SC, Davis IW, Arendall WB, de Bakker PIW, Word JM, Prisant MG, Richardson JS, Richardson DC. 2003. Structure validation by ϕ , ψ and C β deviation. *Proteins* 50:437–450. <http://dx.doi.org/10.1002/prot.10286>.
 42. Rao ST, Rossmann MG. 1973. Comparison of super-secondary structures in proteins. *J Mol Biol* 76:241–256. [http://dx.doi.org/10.1016/0022-2836\(73\)90388-4](http://dx.doi.org/10.1016/0022-2836(73)90388-4).
 43. Hernández-Ortega A, Lucas F, Ferreira P, Medina M, Guallar V, Martínez AT. 2011. Modulating O₂ reactivity in a fungal flavoenzyme: involvement of aryl-alcohol oxidase Phe-501 contiguous to catalytic histidine. *J Biol Chem* 286:41105–41114. <http://dx.doi.org/10.1074/jbc.M111.282467>.
 44. Fernández IS, Ruiz-Duenas FJ, Santillana E, Ferreira P, Martínez MJ, Martínez ÁT, Romero A. 2009. Novel structural features in the GMC family of oxidoreductases revealed by the crystal structure of fungal aryl-alcohol oxidase. *Acta Crystallogr D Biol Crystallogr* 65:1196–1205. <http://dx.doi.org/10.1107/S0907444909035860>.
 45. Record E, Punt PJ, Chamkha M, Labat M, van den Hondel CA, Asther M. 2002. Expression of the *Pycnoporus cinnabarinus* laccase gene in *Aspergillus niger* and characterization of the recombinant enzyme. *Eur J Biochem* 269:602–609. <http://dx.doi.org/10.1046/j.0014-2956.2001.02690.x>.
 46. Mekmouche Y, Zhou S, Cusano AM, Record E, Lomascolo A, Robert V, Simaan AJ, Rousselot-Pailley P, Ullah S, Chaspoul F. 2014. Gram-scale production of a basidiomycetous laccase in *Aspergillus niger*. *J Biosci Bioeng* 117:25–27. <http://dx.doi.org/10.1016/j.jbiosc.2013.06.013>.
 47. Turbe-Doan A, Arfi Y, Record E, Estrada-Alvarado I, Levasseur A. 2013. Heterologous production of cellobiose dehydrogenases from the basidiomycete *Coprinopsis cinerea* and the ascomycete *Podospora anserina* and their effect on saccharification of wheat straw. *Appl Microbiol Biotechnol* 97:4873–4885. <http://dx.doi.org/10.1007/s00253-012-4355-y>.
 48. Varela E, Guillén F, Martínez ÁT, Martínez MJ. 2001. Expression of *Pleurotus eryngii* aryl-alcohol oxidase in *Aspergillus nidulans*: purification and characterization of the recombinant enzyme. *Biochim Biophys Acta* 1546:107–113. [http://dx.doi.org/10.1016/S0167-4838\(00\)00301-0](http://dx.doi.org/10.1016/S0167-4838(00)00301-0).
 49. Fraaije MW, Veeger C, Van Berkel WJ. 1995. Substrate specificity of flavin-dependent vanillyl-alcohol oxidase from *Penicillium simplicissimum*. *Eur J Biochem* 234:271–277. http://dx.doi.org/10.1111/j.1432-1033.1995.271_c.x.
 50. Martínez AT, Speranza M, Ruiz-Duenas FG, Ferreira P, Camarero S, Guillén F, Martínez MJ, Gutiérrez A, de Rio JC. 2005. Biodegradation of lignocellulosics: microbial, chemical, and enzymatic aspects of the fungal attack of lignin. *Int Microbiol* 8:195–204.
 51. Akileswaran L, Brock BJ, Cereghino JL, Gold MH. 1999. 1,4-Benzoquinone reductase from *Phanerochaete chrysosporium*: cDNA cloning and regulation of expression. *Appl Environ Microbiol* 65:415–421.
 52. Brock BJ, Gold MH. 1996. 1,4-Benzoquinone reductase from the basidiomycete *Phanerochaete chrysosporium*: spectral and kinetic analysis. *Arch Biochem Biophys* 331:31–40. <http://dx.doi.org/10.1006/abbi.1996.0279>.
 53. Hammel KE, Kapich AN, Jensen KA, Jr, Ryan ZC. 2002. Reactive oxygen species as agents of wood decay by fungi. *Enzyme Microb Technol* 30:445–453. [http://dx.doi.org/10.1016/S0141-0229\(02\)00011-X](http://dx.doi.org/10.1016/S0141-0229(02)00011-X).